

Densification of rare-earth (Lu, Gd, Nd)-doped alumina nanopowders
obtained by a sol–gel route under seeding

Atsushi Odaka ^a, Tomohiro Yamaguchi ^{a,*}, Takayuki Fujita ^b, Seiichi Taruta ^a
and Kunio Kitajima ^a

^a Department of Chemistry and Material Engineering, Faculty of
Engineering, Shinshu University, 4-17-1 Wakasato, Nagano-shi, 380-8553

^b Taimei Chemicals Co. Ltd., Minamiminowa-mura, Kamiina-gun, Nagano,
399-4597

*Corresponding author:

Tomohiro Yamaguchi

E-mail: mtmouth@shinshu-u.ac.jp

Tel: +81-26-269-5417

Fax: +81-26-269-5415

Abstract

Rare-earth (RE: Lu, Gd, Nd, 0.10 mol%)-doped alumina nanopowders were prepared by a new sol-gel route using polyhydroxoaluminum (PHA) and RECl_3 solutions under α -alumina (~ 75 nm) seeding. Among the rare-earth dopants studied, Lu yields the most suitable nanopowders for low-temperature densification. The 0.10 mol% Lu-doped nanopowders, which were obtained at a calcination temperature of 900°C under 5 mass% α -alumina seeding, consisted of ~ 80 -nm α -alumina particles and γ -alumina nanoparticles. Using these Lu-doped alumina nanopowders, fully densified alumina ceramics with a uniform microstructure composed of fine grains with an average size of $0.61\ \mu\text{m}$ could be obtained at 1400°C by pressureless sintering. Clearly, the Lu-doped nanopowders obtained here represent a viable option for fabricating dense, finer-grained alumina ceramics because an undoped sample with 5 mass% seeds gave a microstructure with an average grain size of $1.78\ \mu\text{m}$ at 1400°C .

Keywords: Alumina; Nanopowders; Sol-gel; Lu-doping; Densification; Grain size

1. Introduction

Properties of alumina ceramics, such as mechanical, electrical and optical properties, are determined by their microstructure (grain size). Thus, the refinement of alumina powder processing techniques is key to obtaining a fine-grained microstructure. Recently, nanopowders such as transition alumina [1, 2], Mg²⁺-doped γ -alumina [3] and nano-grained α -alumina [4-6] powders have attracted much attention as starting raw powders for fabricating dense, finer-grained alumina ceramics, because they have intrinsic nanocrystalline nature. Doping of alumina ceramics has become an effective method of tailoring grain size and shape and grain boundary structure.

We have shown that the use of M²⁺-doped γ -aluminas [3, 7, 8] synthesized through a polyhydroxoaluminum (PHA) sol-gel process [9-11] yields a fine grain size upon sintering due to the intimate mixing of dopants at an atomic level. Among the divalent cation dopants reported in our previous study, Ca²⁺ is by far the best dopant for suppressing the grain growth of α -alumina upon heating [7]. The addition of α -alumina seeds provides multiple low-energy sites for nucleation [8, 12], which allows early impingement of the growing α -alumina colonies, and hence, full densification at lower temperatures. In fact, the use of Ca-doping along with α -alumina seeding was demonstrated to be very effective in producing low-temperature densifiable nanopowders [8].

In our search for more effective dopant species for suppressing grain growth, we have focused on the use of rare-earth (RE)-doping, such as Lu³⁺, Gd³⁺ and Nd³⁺, into γ -alumina. RE elements are used in engineering ceramics and RE-doped alumina ceramics [13-15] have been reported, for example, in connection with the improvement of high-temperature creep resistance [13]. The Lu³⁺ cation has the smallest size (0.861 Å) among the lanthanoids owing to the so-called lanthanoid contraction effect. Thus, the Lu³⁺ cation is smaller than that of Ca²⁺ (1.00 Å) despite its larger atomic number. This suggests that small amount (~0.10 mol%) of Lu³⁺ may be incorporated into the defect γ -alumina spinel lattice, as was the case in the Ca-doping system [7]. However, studies on the effect of dopants on the densification and microstructural evolution of RE-doped alumina nanopowders prepared from the sol-gel process have been lacking, although the role of RE-doped γ -aluminas have been extensively studied in relation to catalytic properties and thermal durability [16-18].

In the present study, RE-doped alumina nanopowders were prepared through the PHA sol-gel route under α -alumina seeding. In order to improve the homogeneity of the seed distribution, seeding was performed during the PHA sol-gel process. Planetary ball milling was also employed to allow further deagglomeration. The objectives of the present study were (i) to investigate the densification behaviour of high-purity RE-doped nanopowders obtained through sol-gel during conventional pressureless sintering, (ii) to compare the suppression effect of Lu³⁺ and Ca²⁺ dopants on

grain growth, and (iii) to demonstrate that PHA-derived Lu-doped nanopowders represent another viable option for achieving full densification with a finer-grained microstructure.

2. Experimental

A high-purity PHA solution was prepared by dissolving Al metal in HCl solution with paying special attention to the impurities [8, 19]. The Al_2O_3 concentration and OH/Al ratio of the final PHA solution thus obtained were determined to be 23.7 mass% and 2.50, respectively, based on the chemical analysis of Al and Cl. An RE chloride such as $\text{LuCl}_3 \cdot 6\text{H}_2\text{O}$ (Kanto Chemical, Japan), used as the RE source, was dissolved in distilled water. The α -alumina powder used for seeding was prepared from commercial α -alumina powder (TM-DAR, Taimei Chemicals, Japan) by planetary ball milling in ethanol for 24 h. The RE chloride solution was added to the PHA solution under an α -alumina seed content of 5 mass% to form a 0.10 mol% RE^{3+} against the mole of Al_2O_3 obtained from the PHA solution. As reference samples, seeded and non-seeded PHA solutions without RE-dopant were also prepared.

The solution mixtures were stirred thoroughly and ultrasonicated. Then, the seeded sols were rapidly dried at 80°C to prevent the segregation of seeds using a large rectangular vat, resulting in the formation of the gels having the thickness of ~2 mm. The gels were ground into <150- μm powders using a high-purity alumina mortar and pestle and then calcined at 700-900°C for 3 h. The calcined powders were deagglomerated again by planetary ball milling in ethanol, followed by slip casting into disks ($\phi = 13$ mm, $t \approx 3$ mm) using gypsum mould, and dried at 120°C. The milled powders will hereafter be abbreviated as, for example, PA-S-Lu0.1(900) and PA-S(900) for the PHA-derived alumina powder with 0.10 mol% Lu^{3+} -dopant and without dopant, respectively, where the calcination temperature (°C) of the doped gels is shown in parentheses. Part of the PA-S-Lu0.1(900) and PA-S(900) powders was uniaxially pressed at 300 MPa for comparison. The amounts of impurities (by mass), as measured by ICP after dissolution, in PL-S-Lu0.1(900), for example, were 10 ppm Si, 9 ppm Na, 4 ppm Mg and 26 ppm Fe, showing that the purity was higher than 99.99%.

To deduce the phase transformation temperature, DTA (TG8120: Rigaku Co., Ltd.) measurements were conducted at a heating rate of 10°C/min under flowing air, using 25-mg powder samples. The phases before and after calcination and the α -fraction were determined by XRD using monochromatic CuK_α radiation (RINT2000: Rigaku Co., Ltd.). The disk-shaped samples obtained by slip casting were sintered at 1200-1500°C for 1 h in air. For comparison, the same temperature-time schedule to that of Ca-doped alumina nanopowders [8] were employed: a heating rate of 50°C/min (below 1300°C) and 12°C/min (above 1300°C) was employed, paying special attention to preventing overshoot at the predetermined

temperature. A cooling rate of 17°C/min was employed down to 300°C. The bulk density of the sintered samples was measured by the Archimedes method. The raw powders and the microstructure of their sintered specimens were characterized by a Hitachi S-3100H scanning electron microscope (SEM), JEOL JEM 2010 transmission electron microscope (TEM) and Hitachi H-2000 scanning transmission electron microscope (STEM) equipped with EDX. TEM samples were prepared by suspending the lightly ground powders in ethanol and evaporating a droplet onto a microgrid. STEM samples were prepared by ion-beam milling. The average grain size of the powders was measured one by one, and the arithmetic average was taken. The average grain size of the sintered samples was estimated by the line-intercept method using at least 150 grain measurements.

3. Results and discussion

3.1 Preparation of RE-doped alumina nanopowders

RE-doped samples obtained at 900°C without seeding consisted of γ -alumina with a trace of χ -alumina, but the χ -alumina tended to disappear with increasing RE content up to 0.50 mol%, as was the case for the M^{2+} doping system [7]. In addition, the exothermic DTA peak temperature (P_m), which deduces the γ -to- α transformation temperature [7], of RE-doped samples increased with increasing dopant content. For example, the order of P_m for 0.30 mol% RE-doped samples without seeding was undoped (1151°C) < Lu-doped (1180°C) < Gd-doped (1198°C) < Nd-doped (1214°C). The order of P_m seems to correspond to the order of ionic size of the RE dopants: a larger dopant cation tends to retard the γ - α transformation, showing a similar trend reported by Kumar et al. [17]. The shift of P_m to higher temperatures due to doping seems to suggest that dopants might be substituted into the defect spinel lattice of γ -alumina, when the dopant amount was as low as 0.10 mol%, as was the case in the Ca^{2+} doping system [8]. Intensive studies on the variation of lattice constant with increasing dopants couldn't reveal the clear evidence of the increase in lattice constant. Nevertheless, the smallest Lu^{3+} cations were considered to be soluble up to 0.10 mol% while larger dopants such as Gd^{3+} and Nd^{3+} might predominantly surface-segregate on γ -alumina particles.

The average grain size of the seeds as determined by TEM is ~75 nm, however, there is a trace amount (estimated to be ~6% at most) of smaller agglomerated particles, which presumably resulted from the abrasion of the high-purity alumina milling media. The average size of the seed particles, as determined from the specific surface area (24.7 m²/g), was 61 nm; this is in good agreement with the value estimated from the TEM micrograph [8].

Without seeding, inevitable grain growth of α -alumina particles occurred from PHA-derived gels with developing 'vermicular' microstructure of aggregates, because the γ -to- α transformation up to ~90% was needed to heat at higher temperature above 1050°C for prolonged time. Therefore, the

seeding is indispensable to obtain well-dispersed alumina nanopowders from the PHA-derived gels.

Table 1 summarizes the powder characteristics of the seed and PA-series powders used for sintering. The powders PA-S(900) and PA-S-Lu0.1(900) transformed into ~90% α -Al₂O₃, while PA-S-Lu0.1(800) and PA-S-Lu0.1(700) powders had an α fraction of 65% and 43%, respectively. The change in BET surface area for these PA-S-Lu series powders corresponded well with the change in the α -fraction. Despite of different γ - α transformation behaviours among Lu-, Gd- and Nd-doped samples, PA-S-Gd0.1(900) and PA-S-Nd0.1(900) powders also exhibited ~90% α -Al₂O₃ transformation, showing that the effect of seeding on the γ - α transformation became predominant at 900°C. Preliminary studies on densification of PA-S-Lu0.1(900), PA-S-Gd0.1(900) and PA-S-Nd0.1(900) powders at 1350°C for 1 h showed a relative density of 97.7%, 92.8% and 92.5%, respectively. Therefore, we focused mainly on the densification of the Lu-doping system.

The TEM micrographs of PA-S(900) and PA-S-Lu0.1(900) powders in Fig. 1 show that the average grain size of α -alumina particles is ~80 nm and that the two powders used for sintering have similar nanoparticle size distributions. The narrow α -alumina particle size distribution probably resulted from the predominant transformation subsystem induced by homogeneously dispersed 5 mass% seeds in the whole powder system [20]. All the powder samples studied here, including PA-S-Gd0.1 and PA-S-Nd0.1 series, were intrinsically nano-sized alumina powders although they did not consist of a single phase. However, the nanopowders calcined at 700-900°C, especially the PA-S-Lu0.1(900) powder, showed excellent low-temperature densification, as discussed in the next section.

3.2 Fabrication of fine-grained alumina ceramics

The densification curves of the PA-S and PA-S-Lu0.1 powders calcined at different temperatures are shown in Fig. 2. The calcination temperature significantly influences the densification behaviour of PA-S-Lu0.1 powders; the temperature at which full densification is attained decreases as the calcination temperature increases. PA-S(900) sintered to 97% relative density at 1300°C and reached >99% at 1375°C. On the other hand, PA-S-Lu0.1(900) sintered to 81% relative density at 1300°C and reached 99.0% at 1400°C. However, the PA-S-Gd0.1(900) and PA-S-Nd0.1(900) powders exhibited a relative density of 98.4% and 97.4%, respectively, when sintered at 1400°C for 1 h: densification of >99% couldn't be achieved even at 1500°C for 1 h for PA-S-Gd0.1(900) and PA-S-Nd0.1(900) powders. This again indicates that Lu-doping leads to the lowest-temperature full densification among the RE dopants studied here. Thus, as suggested by Rani et al. [14] for Yb³⁺, Er³⁺ and La³⁺-doping, it is assumed that inhibition of densification rate depends on the radii of doped cations; the smaller the ionic radii, the better the densification rate.

The commercial δ (35%)/ α -alumina(65%) mixture (green density: 59%)

sintered to only 88% relative density at 1400°C for 0.5 h, with higher grain growth: sintering temperatures >1600°C were required to reach full density [1]. The PA-S-Lu0.1(800) powder, which has a comparable α -alumina fraction and lower green density of 40%, sintered to >98% relative density at 1400°C for 1 h. This indicates that the PA-S-Lu0.1(800) powder, despite of Lu-doping, exhibits lower-temperature densification than the commercial δ/α -alumina powder because the α -alumina nanoparticles in the PA-S-Lu0.1(800) powder were finer. This also demonstrates that the enhanced nano-sized nature of the α -alumina particles in PA-S-Lu0.1 powders is the key to low-temperature densification [4].

Figure 3 shows SEM fractographs of PA-S(900) and PA-S-Lu0.1(900) samples sintered at 1200°C. Both samples have completely transformed into α -alumina. PA-S(900) has undergone slight grain coarsening (130 nm), while PA-S-Lu0.1(900) mostly retains its nanoparticle nature (average grain size: 88 nm). The α -alumina grain size decreased with Lu-doping due to the segregation of the Lu dopant to the grain boundary and grain surface upon heating, while the number of entrapped pores in the sintered specimens increased.

The SEM micrographs of PA-S(900) and PA-S-Lu0.1(900) sintered at 1350 and 1400°C are shown in Fig. 4. The samples were polished and thermally etched before observation. The samples sintered to high densities and developed equiaxed grains. A more homogenous finer-grained (0.61 μm) microstructure was obtained at 1400°C from PA-S-Lu0.1(900) nanopowders (Fig. 4(d)).

Fig. 5 shows the STEM image and the Lu $L\alpha$ line profile of PA-S-Lu0.1(900) sintered at 1400°C. The profile indicates that the doped Lu^{3+} cations segregate in the vicinity of the grain boundary in alumina ceramics. Yoshida et al. [21] also demonstrated that Lu^{3+} ions segregate to Al_2O_3 grain boundaries without forming any secondary phase in 0.10 mol%-doped alumina ceramics sintered at 1400°C with grain size of 0.9 μm , using HRTEM. Therefore, segregation of Lu^{3+} cations at grain boundaries without secondary phase precipitation probably occurred in PA-S-Lu0.1(900) sintered specimens. Li and Ye [6] reported that alumina nanoceramics obtained from α -alumina nanopowders (mean particle size: 10 nm) exhibited a much finer grain size of about 80 and 150 nm at 1450°C and 1500°C, respectively, however, the relative densities remained below 95%. Thus, it is clear that the PA-S-Lu0.1(900) powder is very effective for achieving low-temperature full densification with a finer microstructure.

Both PA-S(900) and PA-S-Lu0.1(900) yielded high densities at 1500°C, but resulted in a greatly coarser-grained microstructure without abnormal grain growth. The average grain size of the sintered PA-S(900) and PA-S-Lu0.1(900) samples was 7.0 and 2.7 μm , respectively, which indicates that the Lu^{3+} dopant retained its suppression effect. However, microstructure observation of PA-S-Lu0.1(900) specimens showed that a little precipitation of the secondary phase (LuAlO_3) at triple points of grains,

which was confirmed by EPMA mapping analysis. This showed that the excess Lu at the grain boundaries precipitates after supersaturation with increasing grain growth.

Recently, Yoshida et al. showed that the segregated dopant effect (0.1 mol%, Mg, Lu, Ti, etc.) on the grain boundary diffusivity in alumina ceramics (sintered at 1400°C for 1 h) was related to the ionicity in the vicinity of the grain boundaries using a first-principle molecular orbital calculation by DV-X α method [22]: the improved ionicity presumably suppressed the atomic diffusion through the increase in the O anion size. They reported that the ionicity around dopants in the vicinity of grain boundaries increased in the order Mg<Sr<Lu, i.e., that the dopant Lu³⁺ had the lowest grain boundary diffusivity. This could explain the retardation of densification of PA-S-Lu0.1(900) specimens, compared with PA-S(900) specimens, and the suppression effect of Lu³⁺ cations on grain growth in PA-S-Lu powders as well. This considerable decrease in grain size is believed to be due to solute drag effect of segregated Lu³⁺ ions on the grain boundary mobility [23].

As in the case of seeded boehmite [20, 24, 25], the number frequency and dispersion homogeneity of α -alumina seeds in PA-S-Lu precursor gels is the key parameter controlling the size of the α -alumina grains, which in turn significantly affects the low-temperature sintering behaviour. Thus, the low-temperature densification behaviour of PA-S-Lu powders forming a finer-grained microstructure is the result of the synergistic effect between the α -alumina nanoparticles and Lu³⁺-dopant, which segregates to the grain boundaries during the transformation/sintering.

The average grain size of PA-S(900) and PA-S-Lu0.1(900) samples is plotted against sintering temperature in Fig. 6, along with the data on PA-S-Ca0.1(900) reported previously [8]. The average grain size of the PA-S(900) samples gradually increased up to 1300°C, followed by marked grain growth at 1350°C. Meanwhile, the average grain size of the PA-S-Lu0.1(900) sample increased gradually up to 1400°C, reaching a grain size of only 0.61 μ m. Comparison of the suppression effect of Ca²⁺ and Lu³⁺ dopants on grain growth indicates that Lu³⁺ is more suppressive than Ca²⁺ dopant reported previously [8], since the sintering conditions and green density were almost identical in both doping systems. The sintering temperature for full densification of PA-S-Ca0.1(900) was 1375°C [8], which was 25°C lower than that of Pa-S-Lu0.1(900). These results suggest that the grain boundary diffusivity in the Lu-doped specimen is lower than that in the Ca-doped specimen.

Our preliminary study showed that the seed content and Lu-doping level had a slight effect on the α -alumina particle size when calcination was performed at 900°C. This shows that the suppression effect of the Lu³⁺ dopant occurred mainly in the sintering stage at higher temperatures, during which the Lu dopant that segregated to the grain boundaries retarded densification and grain growth. The PA-series powders obtained at the calcination temperature of 700°C, especially Nd³⁺- and Gd³⁺-doped series

powders, had poorer lower-temperature sinterability. This resulted mainly from the higher γ -alumina content, which led to decrease in the green density and retardation of the γ - α transformation.

For comparison, a green pellet of the PA-S-Lu0.1(900) sample obtained by uniaxial pressing was sintered at 1400°C under the same sintering conditions. A relative density of 97.5% was obtained. This was lower than the density obtained by slip casting (99.0%), which indicated the advantage of slip casting over uniaxial pressing as a forming method. This can be ascribed to a better homogeneity of particle packing due to an optimal dispersion of particles in the slurry [26]: the green body of uniaxially pressed samples had some large agglomerates, which caused inhomogeneity of particle packing, due to the use of the slurry drying process. Li and Ye [6] pointed out that, in pressureless sintering, a green body having a higher density and smaller pores easily densified into a dense nanoceramic when sintered at the same temperature and for the same duration time. Thus, further study to increase green density by slip casting is needed to attain full density with a finer microstructure at lower temperatures. Therefore, investigations on the effect of slip casting conditions, including the use of appropriate dispersants, on densification and the selection of the optimal co-dopants and sintering conditions, including a two-step sintering method [6], is now underway.

4. Conclusions

In order to fabricate fully densified, fine-grained alumina ceramics, rare-earth (RE: Lu, Gd, Nd, 0.10mol%)-doped alumina nanopowders were prepared through a sol-gel route using a RE-doped PHA solution under seeding. The nanopowders thus obtained, in particular the Lu-doped powders, exhibited excellent low-temperature densification with achieving a finer microstructure owing to the synergistic effect between the nano-sized nature of the α -alumina particles and the suppression effect on grain growth by the homogeneously segregated Lu-dopant to the grain boundaries. The PA-S-Lu0.1(900) samples yielded a relative density of 99.0% with an average grain size of 0.61 μm when sintered at 1400°C for 1 h by conventional pressureless sintering. These results suggest that the new sol-gel method, which employs a Lu-doped PHA solution under seeding, is another viable route for producing low-temperature densifiable alumina nanopowders and would help us towards the fabrication of nanocrystalline alumina ceramics.

References

- [1] C.S. Nordahl, G.L. Messing, Sintering of α -Al₂O₃-seeded nanocrystalline γ -Al₂O₃ powders, *J. Eur. Ceram. Soc.* 22 (2002) 415-422.
- [2] P. Bowen, C. Carry, D. Luxembourg, H. Hofmann, Colloidal processing and sintering of nanosized transition aluminas, *Powder Technol.* 157 (2005) 100-107.
- [3] M. Hida, Y. Yajima, T. Yamaguchi, S. Taruta, K. Kitajima, Fabrication of submicron alumina ceramics by pulse electric current sintering using Mg²⁺-doped transition alumina powders, *J. Ceram. Soc. Japan*, 114 (2006) 184-188.
- [4] X. Sun, J. Li, F. Zhang, X. Qin, Z. Xiu, H. Ru, J. You, Synthesis of nanocrystalline α -Al₂O₃ powders from nanometric ammonium aluminum carbonate hydroxide, *J. Am. Ceram. Soc.* 86 (2003) 1321-1325.
- [5] C.-L. Huang, J.-J. Wang, C.-Y. Huang, Sintering behavior and microwave dielectric properties of nano alpha-alumina, *Mater. Lett.* 59 (2005) 3746-3749.
- [6] J. Li, and Y. Ye, Densification and grain growth of Al₂O₃ nanoceramics during pressureless sintering, *J. Am. Ceram. Soc.* 89 (2006) 139-143.
- [7] A. Odaka, T. Yamaguchi, T. Fujita, S. Taruta, K. Kitajima, Cation dopant effect on phase transformation and microstructural evolution in M²⁺-substituted γ -alumina powders, *J. Mater. Sci.* 43 (2008) 2713-2720.
- [8] A. Odaka, T. Yamaguchi, T. Fujita, S. Taruta, K. Kitajima, Densification of Ca-doped alumina nanopowders prepared by a new sol-gel route with seeding, *J. Eur. Ceram. Soc.* 28 (2008) 2479-2485.
- [9] Y. Yajima, M. Hida, S. Taruta, K. Kitajima, Pulse electric current sintering and strength of sintered alumina using transition alumina powders prepared from polyhydroxoaluminum gel, *J. Ceram. Soc. Japan* 111 (2003) 110-116.
- [10] Y. Yajima, M. Hida, S. Taruta, K. Kitajima, Pulse electric current sintering and strength of sintered alumina using γ -alumina powders prepared by the sol-gel method, *J. Ceram. Soc. Japan* 111 (2003) 419-425.
- [11] M. Hida, Y. Yajima, T. Yamaguchi, S. Taruta, K. Kitajima, Pulse electric current sintering of transition alumina/zirconia composite powders prepared by a novel sol-gel route, *J. Ceram. Soc. Japan* 113 (2005) 543-549.
- [12] J. Tartaj, J. Zárata, P. Tartaj, E.E. Lachowski, Sol-gel cyclic self-production of α -Al₂O₃ nanoseeds as a convenient route for the low cost preparation of dense submicronic alumina sintered monoliths, *Adv. Eng. Mater.* 4 (2002) 17-21.
- [13] H. Yoshida, Y. Ikuhara, T. Sakuma, High-temperature creep resistance in rare earth-doped fine-grained Al₂O₃, *J. Mater. Res.* 13 (1998) 2597-2601.

- [14] D.A. Rani, Y. Yoshizawa, K. Hirao, Y. Yamauchi, Effect of rare-earth dopants on mechanical properties of alumina, *J. Am. Ceram. Soc.* 87 (2004) 289-292.
- [15] G.D. West, J.M. Perkins, M.H. Lewis, The effect of rare earth dopants on grain boundary cohesion in alumina, *J. Eur. Ceram. Soc.* 27 (2007) 1913-1918.
- [16] J.S. Church, N.W. Cant, D.L. Trimm, Stabilization of aluminas by rare earth and alkaline earth ions, *Appl. Catal. A-Gen.* 101 (1993) 105-116.
- [17] K.-N.P. Kumar, J. Tranto, J. Kumar, J.E. Engell, Pore-structure stability and phase transformation in pure and M-doped (M = La, Ce, Nd, Gd, Cu, Fe) alumina membranes and catalyst supports, *J. Mater. Sci. Lett.* 15 (1996) 266-270.
- [18] M. Ozawa, Y. Nishio, Thermal stabilization of γ -alumina with modification of lanthanum through homogeneous precipitation, *J. Alloy. Compd.* 374 (2004) 397-400.
- [19] T. Fujita, K. Kitajima, S. Taruta, N. Takusagawa, Chemical species in polyaluminum hydroxide solution, *Nippon Kagaku Kaishi* (1993) 319-328.
- [20] F.S. Yen, H.S. Lo, H.L. Wen, R.J. Yang, θ - to α -phase transformation subsystem induced by α - Al_2O_3 -seeding in boehmite-derived nano-sized alumina powders, *J. Cryst. Growth* 249 (2003) 283-293.
- [21] H. Yoshida, Y. Ikuhara, T. Sakuma, Improvement of creep resistance in polycrystalline Al_2O_3 by Lu-doping, *Int. J. Inorg. Mater.* 1 (1999) 229-234.
- [22] H. Yoshida, S. Hashimoto, T. Yamamoto, Dopant effect on grain boundary diffusivity in polycrystalline alumina, *Acta Mater.* 53 (2005) 433-440.
- [23] A. Altay, M.A. Gülgün, Microstructural evolution of calcium-doped α -alumina, *J. Am. Ceram. Soc.* 86 (2003) 623-629.
- [24] S. Kwon, G.L. Messing, Sintering of mixtures of seeded boehmite and ultrafine α -alumina, *J. Am. Ceram. Soc.* 83 (2000) 82-88.
- [25] K.R. Han, C.S. Lim, M.-J. Hong, J.W. Jang, K.S. Hong, Preparation method of submicrometer-sized α -alumina by surface modification of γ -alumina with alumina sol, *J. Am. Ceram. Soc.* 83 (2000) 750-754.
- [26] M. Azar, P. Palmero, M. Lombardi, V. Garnier, L. Montanaro, G. Fantozzi, J. Chevalier, Effect of initial particle packing on the sintering of nanostructured transition alumina, *J. Eur. Ceram. Soc.* 28 (2008) 1121-1128.

Figure captions

Fig. 1 TEM micrographs of (a) PA-S(900) and (b) PA-S-Lu0.1(900) powders.

Fig. 2 Bulk density of sintered specimens plotted against sintering temperature for PA-S(900) (Δ), PA-S-Lu0.1(900) (\circ), PA-S-Lu0.1(800) (\square) and PA-S-Lu0.1(700) (∇).

Fig. 3 SEM micrographs of (a) PA-S(900) and (b) PA-S-Lu0.1(900) samples sintered at 1200°C.

Fig. 4 SEM micrographs of PA-S(900) samples sintered at 1350°C (a) and 1400°C (b) and PA-S-Lu0.1(900) samples sintered at 1350°C (c) and 1400°C (d).

Fig. 5 (a) STEM micrograph and (b) Lu $L\alpha$ line profile of PA-S-Lu0.1(900) sample sintered at 1400°C. Line analysis was carried out along the line shown in Fig. 5 (a).

Fig. 6 Average grain size plotted against sintering temperature for PA-S(900) (Δ), PA-S-Lu0.1(900) (\circ) and PA-S-Ca0.1(900) (∇) [8].

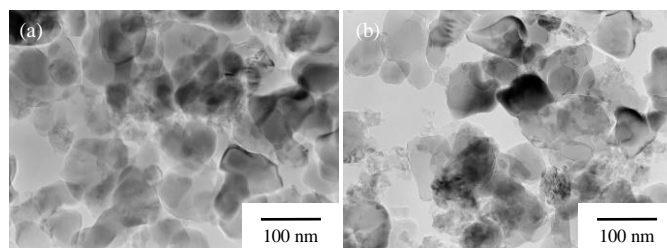


Fig. 1

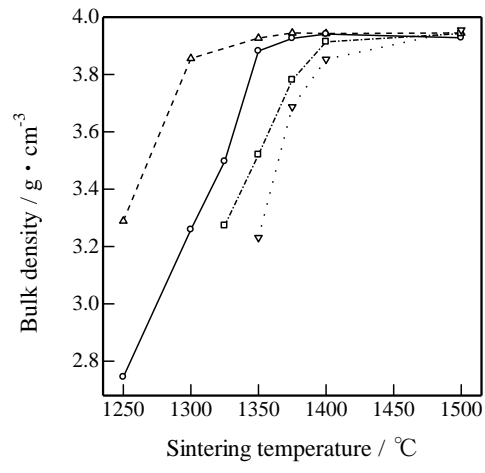


Fig. 2

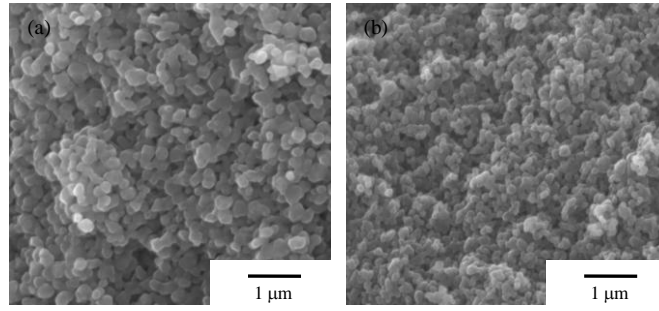


Fig. 3

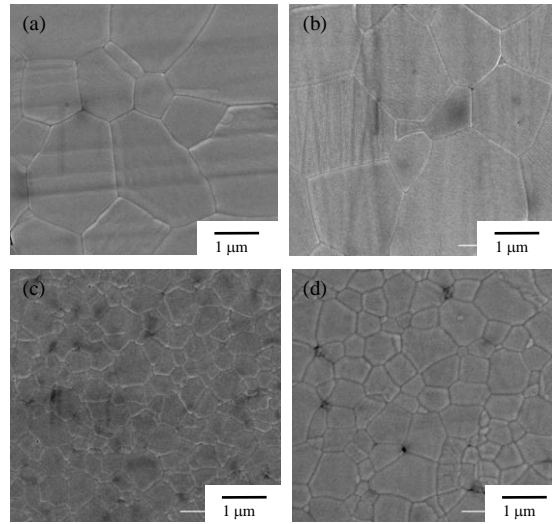


Fig. 4

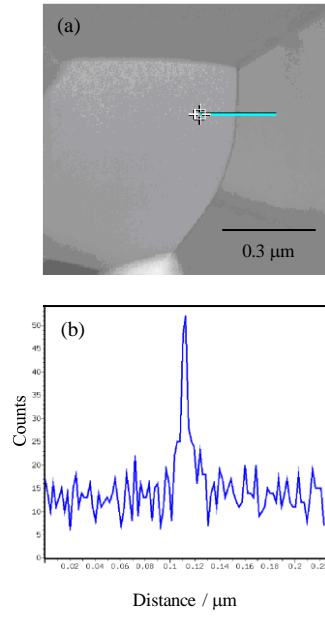


Fig. 5

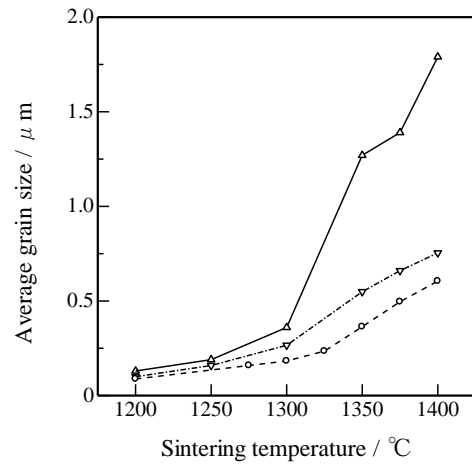


Fig. 6